

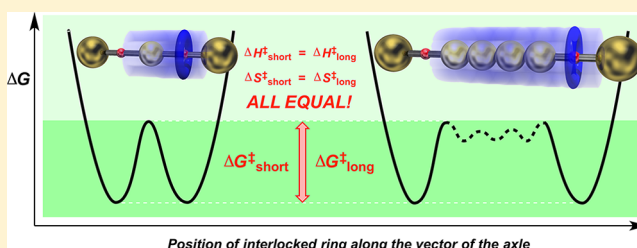
Axle Length Does Not Affect Switching Dynamics in Degenerate Molecular Shuttles with Rigid Spacers

Philip G. Young, Keiji Hirose,* and Yoshito Tobe

Division of Frontier Materials Science, Graduate School of Engineering Science, Osaka University, 1-3 Machikaneyama, Toyonaka 560-8531, Japan

S Supporting Information

ABSTRACT: For a series of [2]rotaxane molecular shuttles possessing linear rigid rod-like axles of varying lengths between degenerate recognition sites, the activation barrier for shuttling motion was clearly shown to be constant. Moreover, dynamic NMR studies have revealed that both the entropic and enthalpic contributions to the shuttling motion remain constant regardless of the actual length of the rigid rod-like axles employed herein.



INTRODUCTION

The potential of mechanically interlocked molecules to function as nanoscale devices has driven their rapid development in recent years.¹ These devices exploit the unique relative motions of molecular components in response to physical or chemical stimuli.² [2]Rotaxanes are composed of a linear molecular axle interpenetrated with a macrocyclic ring.³ Bulky stoppers, placed at each end of the axle, ensure the macrocyclic ring remains interlocked, or mechanically bound. Due to their potential use as molecular switches, much attention has been devoted to [2]rotaxanes that possess two recognition sites, between which the interlocked macrocyclic ring can shuttle.⁴ In such molecular shuttles, the control of ring shuttling along the axle component is of crucial importance, as this kinetic parameter, sometimes referred to as switching rate, may directly determine their effectiveness in a device setting.^{1b,5} It follows that an increased understanding of shuttling motion is an indispensable requirement for the rational design of nanoscale devices.

Although there have been numerous reports on the general effects of the structural features of rotaxanes on ring shuttling, there are relatively few that offer detailed kinetic analyses.⁶ Moreover, there is a distinct absence of research that deals specifically with elucidating the effect of axle length on ring shuttling. Rotaxanes with increasing numbers of flexible axle components, such as poly(ethylene glycol) (PEG) units or straight aliphatic carbon chains, unfortunately have inherent drawbacks as model rotaxanes that render the detailed evaluation of kinetic factors difficult. In such systems, effects arising from conformational isomerism, including loss of conformational freedom during ring shuttling, back-folding,^{6d,j} harpooning,^{6a} or Coulombic repulsion between components,^{2a} can highly complicate ring shuttling. Additional practical complications, such as small spectral changes, spectral complexity,⁶ⁱ or poor solubility,^{6b} add to the abundance of difficulties

involved with the evaluation of entropic contributions to the switching rates both experimentally and computationally.⁷

In order to gain an enhanced understanding of the impact axle length has on the activation barrier to ring shuttling, to increase our ability to rationally design molecular shuttles, kinetic studies using suitable model rotaxanes are indispensable. The rotaxanes we chose to investigate incorporate oligo-(phenylene) spacers that separate two secondary ammonium binding stations (Figure 1, type **1ⁿ**, $n = 1-4$). Two large

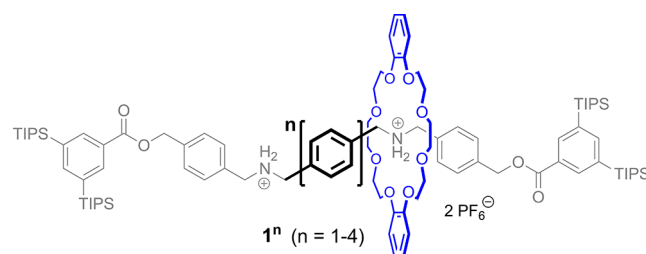


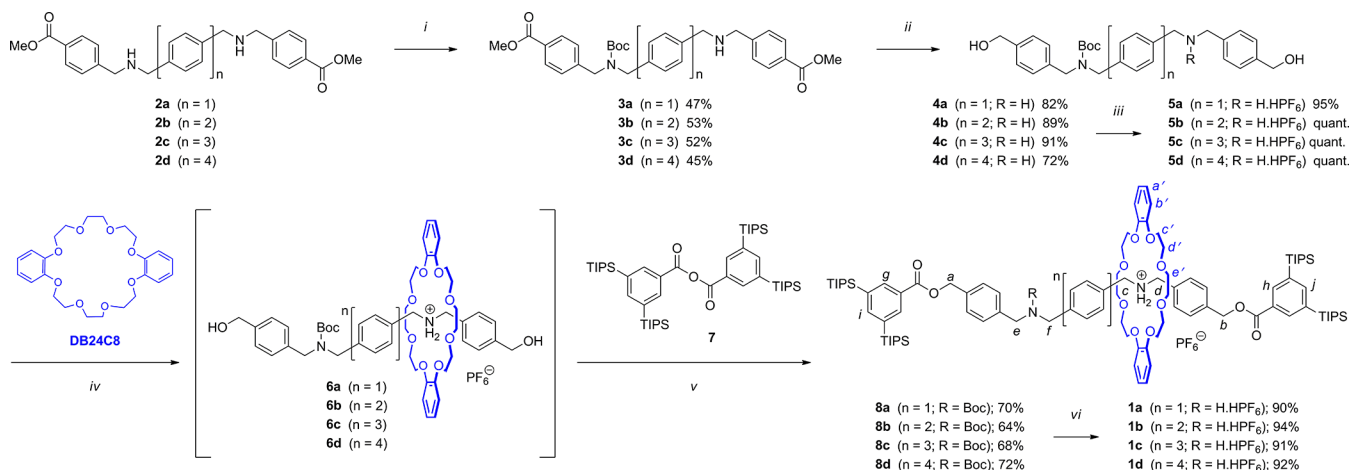
Figure 1. General structures of the [2]rotaxanes investigated.

stoppers, based on 1,3-bis(triisopropylsilyl)benzene, are located at either end of the axle, and an interpenetrated dibenzo-24-crown-8 ether (DB24C8) is able to shuttle between the two charged stations.

Prominent features of rotaxanes **1ⁿ** are the rigid rod-like structures they are expected to sustain, a direct consequence of their aromatic backbones. Thus, by incorporating an increasing number of phenylene spacers in the axle, we are able to systematically extend the distance between the two ammonium stations from 6.9 ($n = 1$) to 19.6 Å ($n = 4$).⁸ As a result of their rigid linear nature, effects arising from conformational isomerism of the axle can be ruled out in **1ⁿ**, thus allowing us to gain

Received: December 13, 2013

Published: May 9, 2014

Scheme 1. Synthesis of the Rigid Rod-Like [2]Rotaxanes Studied^a

^aSee Supporting Information for experimental details of 2a–2d. Reagents and conditions: (i) Boc₂O (1 equiv), 4-dimethylaminopyridine, CH₂Cl₂, rt; (ii) lithium aluminum hydride, THF, 0 °C to rt; (iii) NH₄PF₆, acetone, H₂O; (iv) DB24C8, CH₂Cl₂, –20 °C; (v) 7, *n*-Bu₃P, CH₂Cl₂, –20 °C to rt; (vi) trifluoroacetic acid, CH₂Cl₂, then saturated aqueous NH₄PF₆.

unbiased knowledge of how length influences the activation barrier for ring shuttling. In addition, on the basis of our previous work with structurally related rotaxanes,⁹ rotaxanes of type 1ⁿ are expected to provide clear spectral changes suitable for reliable evaluation of kinetic parameters.

RESULTS AND DISCUSSION

The synthesis of [2]rotaxanes is outlined in Scheme 1. One of the amine centers of the key axle intermediates 2a–2d, in which the central axle aromatic components consist of rigid rod-like oligo(phenylene) groups of varying lengths (see Supporting Information for the synthesis), was protected with a *tert*-butoxycarbonyl (Boc) group by treatment with 1 equiv of di-*tert*-butyl dicarbonate. The presence of a single Boc protecting group will ensure exclusive formation of desired [2]rotaxanes, as opposed to [3]rotaxanes, in the later capping reaction.^{9c,10} Reduction of the resulting methyl esters 3a–3d with lithium aluminum hydride gave diols 4a–4d, which were treated with aqueous ammonium hexafluorophosphate to provide salts 5a–5d. Rotaxane formation was accomplished by the well-established threading-followed-by-capping protocol that involves complex formation of each of the hexafluorophosphate salts 5a–5d with DB24C8 at –20 °C to form pseudorotaxanes 6a–6d, followed by treatment with anhydride stopper 7^{9c} in the presence of *n*-tributyl phosphine.¹¹ The Boc-protected [2]rotaxanes 8a–8d were subsequently treated with trifluoroacetic acid to provide 1a–1d.

The ¹H NMR spectra of rotaxanes 1a–1d in CDCl₃, CDCl₂CDCl₂, CD₃CN, toluene-*d*₈ (Tol-*d*₈), DMF-*d*₇, and DMSO-*d*₆ at 303 K revealed slow shuttling of the DB24C8 ring between the ammonium stations on the time scale of the NMR (see Figure 2 for ¹H NMR spectra of 1a–1d in DMSO-*d*₆). Specifically, all spectra indicated the existence of a nonsymmetrical system with separate sets of signals observed for the complexed and uncomplexed sides of each of the [2]rotaxanes. This slow ring shuttling condition in 1a–1d was best exemplified by the presence of two sharp singlets in the ¹H NMR spectra appearing at approximately 5.4 and 5.3 ppm that were assigned to the nonequivalent benzylic protons H^a and H^b, respectively. The observed slow shuttling can be justified by the strong noncovalent binding interactions between the

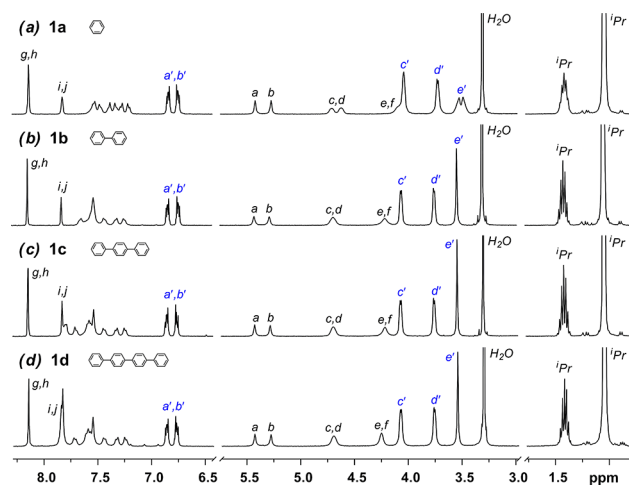


Figure 2. Partial ¹H NMR spectra (400 MHz, DMSO-*d*₆, 303 K) of (a) 1a, (b) 1b, (c) 1c, and (d) 1d. See Scheme 1 for proton assignments.

DB24C8 ring and dibenzylammonium centers of each axle, which result in the localization of the macrocycle around one of the equivalent ammonium centers, thus desymmetrizing the otherwise C_{∞h}-symmetrical system.^{10,12} Notably, ring shuttling remained slow on the NMR time scale in CDCl₃, CDCl₂CDCl₂, CD₃CN, and Tol-*d*₈ up to the temperature limits of each solvent as revealed by the persistence of two sharp singlets for H^a and H^b in variable temperature measurements (Supplementary Figures S48–S51). On the other hand, coalescence of the complexed and uncomplexed signals was observed in DMSO-*d*₆ and DMF-*d*₇ within the temperature limits of these solvents, indicating a significant difference in shuttling behavior between the former nonpolar solvents and these two polar solvents. The lower barriers for the shuttling in DMSO-*d*₆ and DMF-*d*₇ are ascribed to far better solvating ability of the positively charged ammonium centers of each rotaxane, making the solvents more effectively able to compete with the noncovalent interactions with DB24C8 compared to the nonpolar solvents.¹³

Variable-temperature ^1H NMR investigations were carried out in $\text{DMSO-}d_6$ and $\text{DMF-}d_7$ to elucidate the kinetic parameters of the ring shuttling in rotaxanes **1a–1d**. The rates of ring shuttling (k [s^{-1}]) were derived from ^1H NMR line shape analyses (LSA)¹⁴ of the H^a and H^b resonances at increasing temperatures (Supporting Information). As a representative example, shown in Figure 3a and b are

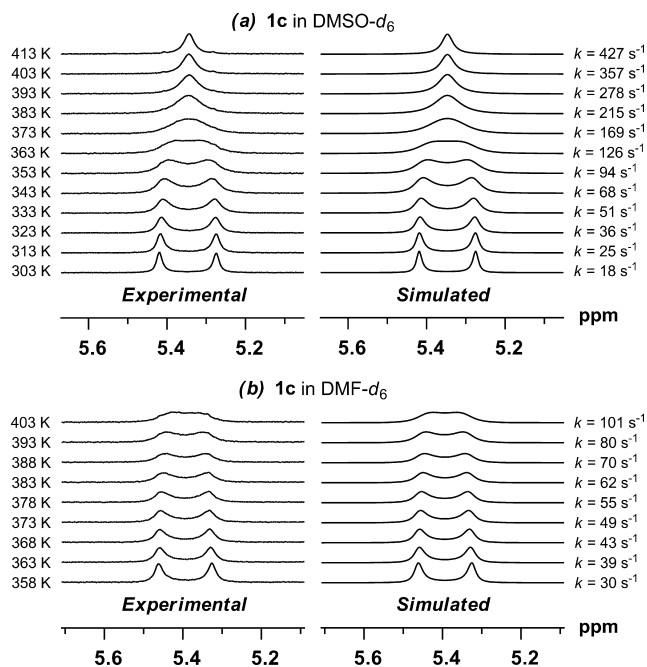


Figure 3. Experimentally determined, simulated variable-temperature ^1H NMR (400 MHz) spectra of H^a and H^b of rotaxane **1c** in (a) $\text{DMSO-}d_6$ and (b) $\text{DMF-}d_7$. For each temperature the calculated rate constants (k) are shown.

experimental, simulated variable-temperature ^1H NMR spectral data of protons H^a and H^b of rotaxane **1c** in $\text{DMSO-}d_6$ and $\text{DMF-}d_7$, respectively. In $\text{DMSO-}d_6$ protons H^a and H^b initially appeared as two sharp singlets at 303 K, with LSA revealing an exchange rate (i.e., shuttling rate [k]) of 18 s^{-1} (Figure 3a). An increase in temperature was accompanied by a gradual broadening of H^a and H^b and a concomitant increase in shuttling rate as indicated by LSA. At 363 K, coalescence of H^a and H^b was observed, which was followed by further sharpening of the newly formed singlet at even higher temperatures. Taken together, these observations indicated a state of slow ($k = 18 \text{ s}^{-1}$ at 303 K) to fast ring shuttling ($k = 427 \text{ s}^{-1}$ at 413 K) on the NMR time scale. In contrast to the observations in $\text{DMSO-}d_6$, in $\text{DMF-}d_7$ H^a and H^b of **1c** remained as two sharp singlets up to 358 K ($k = 30 \text{ s}^{-1}$); coalescence of the signals was not observed until 403 K ($k = 101 \text{ s}^{-1}$, Figure 3b), indicating a substantial difference in shuttling behavior. Similar trends in the

variable temperature ^1H NMR experiments were observed across the series of rotaxanes (see Supplementary Figures S52–S59 for variable temperature spectra).

Based on the rates of ring shuttling derived from ^1H NMR LSA, the free energies of activation (ΔG^\ddagger) for ring shuttling were calculated for **1a–1d** in $\text{DMSO-}d_6$ and $\text{DMF-}d_7$ using the Eyring equation (Supplementary Figures S52–S59). Selected kinetic data for rotaxanes **1a–1d** in $\text{DMSO-}d_6$, $\text{DMF-}d_7$ are summarized in Table 1, respectively. The ΔG^\ddagger values are higher in $\text{DMF-}d_7$ relative to $\text{DMSO-}d_6$ at identical temperatures, which is presumably due to the differences in the abilities of the solvents to solvate the charged ammonium docking stations. Considering the relative Gutmann donor numbers (DN) of each solvent, where the DN for DMSO and DMF are 29.8 and 26.6,¹⁵ respectively, then it becomes clear that ring shuttling is less impeded in solvents that are better able to donate their electrons into noncovalent bonds. Surprisingly, at each given temperature the data show that the activation barriers for ring shuttling are similar for each rotaxane, irrespective of the length of the axle. For instance, at 303 K in $\text{DMSO-}d_6$ the ΔG^\ddagger value for rotaxane **1a**, which contains just one phenylene group between the ammonium stations, is the same as that for **1d**, which contains four phenylene groups between the ammonium stations (cf. $16.0 \text{ kcal mol}^{-1}$). Such assessments of ΔG^\ddagger can also be carried out at higher temperatures in both $\text{DMSO-}d_6$ and $\text{DMF-}d_7$, where the ΔG^\ddagger values show very slight variation. These observations indicate that increasing axle length has no significant impact on the activation barrier of ring shuttling.

In order to gain a deeper understanding of ring shuttling, the kinetic parameters were examined (Table 2). In both $\text{DMSO-}d_6$

Table 2. Summary of Kinetic Properties for **1a–1d** in $\text{DMSO-}d_6$ and $\text{DMF-}d_7$

	$\text{DMSO-}d_6$		$\text{DMF-}d_7$	
	ΔH^\ddagger (kcal mol^{-1})	ΔS^\ddagger ($\text{cal K}^{-1} \text{ mol}^{-1}$)	ΔH^\ddagger (kcal mol^{-1})	ΔS^\ddagger ($\text{cal K}^{-1} \text{ mol}^{-1}$)
1a	6.4 ± 0.2	-32.5 ± 0.6	5.6 ± 0.2	-35.6 ± 0.6
1b	6.4 ± 0.1	-31.3 ± 0.4	6.5 ± 0.3	-33.5 ± 0.6
1c	6.7 ± 0.1	-31.1 ± 0.3	6.1 ± 0.2	-34.9 ± 0.7
1d	6.4 ± 0.2	-31.8 ± 0.5	6.2 ± 0.2	-34.9 ± 0.5

and $\text{DMF-}d_7$ the ΔH^\ddagger parameters for ring shuttling across the series of rotaxanes are on average $6.3 \text{ kcal mol}^{-1}$, regardless of composition of the axle, with a maximum variation of $1.1 \text{ kcal mol}^{-1}$. These findings suggest that the length of the rigid axes has no significant impact on the activation enthalpy. The seemingly static nature of ΔH^\ddagger is proposed to be a consequence of the mutual shuttling mechanism that takes place in each rotaxane. That is, for each rotaxane the fundamental requirement of ring shuttling takes place by the breakage of hydrogen bonds between a **DB24C8** ring and a dibenzylammonium station by solvent coordination. The extent

Table 1. Kinetic Data for Ring Shuttling in $\text{DMSO-}d_6$ and $\text{DMF-}d_7$ for Rotaxanes **1a–1d** Derived from Dynamic NMR Studies

	$\text{DMSO-}d_6$			$\text{DMF-}d_7$	
	$\Delta G^\ddagger_{303 \text{ K}}$ (kcal mol^{-1})	$\Delta G^\ddagger_{353 \text{ K}}$ (kcal mol^{-1})	$\Delta G^\ddagger_{393 \text{ K}}$ (kcal mol^{-1})	$\Delta G^\ddagger_{353 \text{ K}}$ (kcal mol^{-1})	$\Delta G^\ddagger_{393 \text{ K}}$ (kcal mol^{-1})
1a	16.0	17.8	19.1	18.2	19.6
1b	15.8	17.4	18.7	18.3	19.7
1c	16.0	17.6	18.8	18.4	19.8
1d	16.0	17.6	18.9	18.5	19.9

of these hydrogen bond interactions, as well as ion-dipole interactions and π - π interactions between **DB24C8** and each axle in transition states, are thought to be the essentially the same across this series of rotaxanes. Indeed, the average ΔH^\ddagger value of 6.3 kcal mol⁻¹ is consistent with the breakage of moderate [N⁺-H...O] hydrogen-bonding interactions, with any minor π - π interactions between the ring and axle.¹⁶ Though the ring shuttling from one station to the other involves bypassing a different number of phenylene spacers, taking into account that there are no significant changes in steric barriers associated with the number of spacer units present, it is reasonable that there is no significant variation in ΔH^\ddagger .

Considering the consistency of the ΔG^\ddagger values observed for **1a–1d** (Table 1) and the similarity of the activation enthalpies (Table 2), the activation entropies (ΔS^\ddagger) were not expected to play an important role in the determination of ΔG^\ddagger . Indeed Table 2 shows that there is only a slight variation in the ΔS^\ddagger values across this series of rotaxanes in each solvent. In both DMSO-*d*₆ and DMF-*d*₇ average values of ΔS^\ddagger for this series of rotaxanes were found to be -31.7 and -34.7 cal K⁻¹ mol⁻¹ (with maximum variations of 1.4 and 2.1 cal K⁻¹ mol⁻¹), respectively. It is clear from the large negative values of ΔS^\ddagger that ring shuttling involves a great deal of ordering. Indeed, we expect there to be a large entropic effect on ring shuttling based on the breakage and restoration of ion pairs as the ring shuttles between each positively charged center.^{6h,17} Specifically, extensive reordering of the solvent molecules is likely to occur as a result of the hexafluorophosphate counterions becoming essentially “naked” as one dissociates completely from an ammonium center.^{17d} Furthermore, studies by Stoddart and co-workers suggest that the overall rigidity of a rotaxane is increased as a **DB24C8** ring slips over a *p*-phenylene group.^{6h}

Although activation entropy is influenced by many factors,¹⁸ the nonvariation of the activation of entropy in this series of rotaxanes suggests that each rotaxane endures a similar extent of conformational loss in the transition state. Evidently, the actual lengths of the rigid linear rod-like spacer units employed herein have no direct effect on the activation entropy for shuttling, so the system can be described by the steady-state approximation. As previously mentioned, the larger activation barriers in DMF-*d*₇ relative to those in DMSO-*d*₆ are due to the differences in their abilities to solvate the two charged stations. It is clear that these solvent effects manifest themselves in the ΔS^\ddagger parameters, being on average more negative in DMF-*d*₇ than in DMSO-*d*₆. This can be explained by considering a larger penalty will be paid for decomplexation of the **DB24C8** ring from a charged center of a rotaxane in DMF-*d*₇ relative to DMSO-*d*₆. That is, based on their respective dielectric constants, DMF-*d*₇ molecules will become more ordered in the transition state relative to DMSO-*d*₆ molecules. We believe the ordering of these highly polar solvents around the charged ammonium stations in the transition states, as well as the effect of breaking and restoring of ion pairs, gives rise to the large negative values of ΔS^\ddagger for **1a–1d**.

Given the similarities in kinetic parameters across this series of rotaxanes, it is clear that axle length does not significantly influence the rate of ring shuttling. It is worth noting that the lack of spacer length dependence on switching dynamics with our rigid rod-like rotaxanes significantly contrasts that of rotaxanes reported by others. In particular, Brouwer and co-workers have found that the movement of a tetralactam ring

between a succinamide station and a reduced naphthalimide group along flexible carbon chains of varying lengths decreases with increasing axle length.¹⁹ This behavior was originally described by a biased random walk model; however, the origin of the bias was not identified, and the general validity of this model has recently been questioned by new findings.^{6a} An alternative “harpooning” mechanism is proposed to take place in which the macrocyclic ring is simultaneously bound to both stations of the rotaxane, a situation made possible by the flexible carbon linkers present. Brouwer and co-workers’ proposed harpooning mechanism is compatible with the length dependence originally reported since the formation of the transition state structure is less probable as the length of the spacer is increased. Importantly, as the rotaxanes presented herein are composed of rigid rod-like axles, harpooning can be excluded, and the lack of length dependence on shuttling dynamics can be explained. On the basis of the experimental data obtained, it can be proposed that the overriding rate-determining factor is the strong interaction of the **DB24C8** ring with the ammonium stations. In addition to this, a significant amount of energy is required for recomplexation since this would involve the displacement of strongly bound solvent molecules. The amount of free energy required for decomplexation and complexation of the **DB24C8** ring with the ammonium stations is greatest among the free energy barriers associated with the shuttling of the ring along the axle within the length examined in this work. In such a situation the ring most probably moves back and forth along the axle several times before rebinding with equal probability to either of the ammonium ions.

CONCLUSIONS

The detailed analyses of ring shuttling in a family of degenerate molecular shuttles presented herein suggest that axle length has no significant impact on the activation barrier for ring shuttling. On the basis of the similarities of activation enthalpy for **1a–1d**, the number of rigid spacer units bears no consequence on steric barriers for ring shuttling. In addition, the activation entropy showed little variation. It follows that fine-tuning of molecular shuttles may be possible by consideration of the degrees of flexibility present in an axle component. For example, one can imagine that incorporating a long rigid axle in a molecular device will serve as a physical barrier, with defined length, however, such a barrier will not influence the switching rate. These findings strengthen our fundamental understanding of molecular shuttles and will no doubt be of great use to the creators of new functional devices.

EXPERIMENTAL SECTION

General Methods. Melting points were measured with a hot-stage apparatus equipped with a thermometer. ¹H nuclear magnetic resonance (NMR) spectra were recorded at 303 K using a Bruker AVANCEIII-400 at a frequency of 400 MHz or a JEOL JNM-ECS400 at a frequency of 400 MHz and are reported as parts per million (ppm) downfield shift from tetramethylsilane (δ_{H} 0.00) or deuteriochloroform (CDCl₃, δ_{H} 7.26 ppm) as internal references, unless otherwise stated. The data are reported as chemical shift (δ), multiplicity (br = broad, s = singlet, d = doublet, t = triplet, q = quartet, m = multiplet), coupling constant (*J*, Hz), relative integral. ¹³C nuclear magnetic resonance spectra were recorded at 303 K using a Bruker AVANCEIII-400 at a frequency of 100 MHz or a JEOL JNM-ECS400 at a frequency of 100 MHz and are reported as parts per million (ppm) downfield shift from deuteriochloroform (δ_{C} 77.16 ppm) or tetramethylsilane (δ_{C} 0.00) as internal references, unless

otherwise stated. The substitution of carbon signals was determined on the basis of distortionless enhancement by polarization transfer (DEPT) ^{13}C experiments. IR spectra were recorded as a KBr disk or a neat film using a JASCO FT/IR-4200 spectrometer. Low resolution mass spectral analyses (fast atom bombardment [FAB] and electron impact [EI]) were performed by means of a JEOL JMS-700V spectrometer. Low resolution mass spectral analyses (laser desorption [LD]) mass measurements were performed by means of a Shimadzu/Kratos AXIMA-CFR spectrometer. High resolution electrospray ionization spectra were recorded on a JEOL JMS-700V spectrometer. Elemental analyses were carried out by using a Perkin-Elmer 2400II analyzer. Analytical thin layer chromatography (TLC) was performed using precoated silica gel plates (Merck Kieselgel 60 F254). Preparative column chromatography was carried out using Fuji Silysia BW-300 silica gel (SiO_2 ; 0.038–0.075 mm) with the indicated solvents, which were mixed v/v as specified. Compounds **5a**^{9c} and **7**^{9e} were synthesized according to our previously reported procedures. All other reagents were obtained from commercial suppliers and used as received. CH_2Cl_2 and THF were dried by a Glass Contour solvent purification system prior to use.

General Procedure A: Rotaxane Formation. DB24C8 (1.1–1.5 equiv) was added to a suspension of the hexafluorophosphate salt (1 equiv) in dichloromethane (~0.1 M) to give a homogeneous reaction mixture. A solution of anhydride stopper **7** (2.1 equiv) in dichloromethane was then added at $-20\text{ }^\circ\text{C}$ (final concn ~0.05 M) followed by tri-*n*-butylphosphine (0.4 equiv). The mixture was stirred under an atmosphere of nitrogen at $-20\text{ }^\circ\text{C}$ for 3–5 h after which time it was stirred at ambient temperature for 1–2 h. The solvent was then removed under reduced pressure, and the resulting crude product was subjected to column chromatography to give the desired rotaxane (**8a–8d**).

General Procedure B: Boc-Deprotection. Under an atmosphere of nitrogen, trifluoroacetic acid (0.2 mL) was added to a solution of rotaxane (**8a–8d**) in dichloromethane (1 mL). After the reaction mixture was stirred at ambient temperature for 2 h, it was poured onto saturated aqueous NH_4PF_6 (20 mL) and then extracted with dichloromethane ($3 \times 15\text{ mL}$). The combined organics were washed with saturated aqueous NH_4PF_6 (30 mL), dried (MgSO_4), and then concentrated under reduced pressure. The crude product thus obtained was triturated with hexane to provide the desired bis-hexafluorophosphate salt (**1a–1d**).

General Procedure C: Mono Boc-Protection. Under an atmosphere of nitrogen, Boc-anhydride (1 equiv) and N,N -(dimethylamino)-pyridine (0.05 equiv) were added to a solution of diamine (1 equiv) in dichloromethane. The reaction mixture was stirred at ambient temperature for 3 h and was then concentrated under reduced pressure. Purification by column chromatography provided the desired mono-Boc-protected product (**3b–3d**) and the di-Boc-protected product (**9–11**).

General Procedure D: Ester Reduction. Under an atmosphere of nitrogen, a solution of mono-Boc compound (1 equiv) in tetrahydrofuran was added dropwise to a suspension of lithium aluminum hydride (3 equiv) in tetrahydrofuran at $0\text{ }^\circ\text{C}$ over 5 min. The reaction mixture was stirred at $0\text{ }^\circ\text{C}$ for 30 min and then slowly warmed to ambient temperature. After 30 min TLC showed complete consumption of the starting material, and the reaction was quenched with ice-water (30 mL) at $0\text{ }^\circ\text{C}$ and then extracted with $\text{CHCl}_3/\text{PrOH}$ (3:1 v/v, $5 \times 30\text{ mL}$). The combined organic layers were dried (MgSO_4) and then concentrated under reduced pressure. The crude product obtained was subsequently purified by column chromatography to afford the desired diol (**4b–4d**).

General Procedure E: Hexafluorophosphate Salt Formation. Saturated aqueous NH_4PF_6 (1 mL) was added dropwise to a solution of diol (**4b–4d**) in acetone (3 mL). A precipitate immediately formed. Argon gas was then bubbled through the reaction suspension with stirring at ambient temperature for 2 h. The reaction mixture was then concentrated and partitioned between water (20 mL) and $\text{CHCl}_3/\text{PrOH}$ (3:1 v/v, $4 \times 20\text{ mL}$). The combined organic layers were dried (MgSO_4) and then concentrated under reduced pressure to

afford the desired hexafluorophosphate salt (**5b–5d**), which was used in the next step without further purification.

8a. Hexafluorophosphate salt **5a** (50.0 mg, 0.0803 mmol) was treated according to General Procedure A. The crude product was subjected twice to column chromatography (column 1: silica gel, $\text{CHCl}_3/\text{EtOAc}$ [6:1] then $\text{CHCl}_3/\text{CH}_3\text{OH}$ [10:1]; column 2: silica gel, acetone/ CH_2Cl_2 [1:20]) to give the desired rotaxane **8a** as a colorless foam (0.106 g, 70%). $R_f = 0.44$ (acetone/ CH_2Cl_2 [1:20]). Mp $106\text{--}109\text{ }^\circ\text{C}$. ^1H NMR (400 MHz, CDCl_3) δ_{H} (ppm) 8.20 (d, $J = 1.2\text{ Hz}$, 2 H), 8.19 (d, $J = 1.1\text{ Hz}$, 2 H), 7.83 (d, $J = 6.2\text{ Hz}$, 2H), 7.68–7.54 (br m, 2 H), 7.42 (d, $J = 8.1\text{ Hz}$, 2 H), 7.32–7.24 (m, 4 H), 7.24–7.17 (br m, 2 H), 7.12–7.03 (br m, 2 H), 6.85–6.69 (m, 8 H), 5.38 (s, 2 H), 5.29 (s, 2 H), 4.73–4.57 (br m, 4 H), 4.42–4.19 (br m, 4 H), 4.15–4.02 (m, 8 H), 3.86–3.71 (m, 8 H), 3.52 (s, 8 H), 1.52–1.36 (overlapping m, 12 H), 1.47 (s, 9 H), 1.09 (d, $J = 1.0\text{ Hz}$, 36 H), 1.07 (d, $J = 1.0\text{ Hz}$, 36 H). ^{13}C NMR (100 MHz, CDCl_3) δ_{C} (ppm) 167.3 (CO), 167.1 (CO), 156.0 (CO), 147.4 (ArC), 147.2 (ArCH), 147.0 (ArCH), 139.4 (ArC), 137.8 (ArC), 137.0 (ArCH), 136.6 (ArCH), 136.5 (ArCH), 135.7 (ArC), 134.3 (ArC), 134.2 (ArC), 131.4 (ArC), 130.8 (ArC), 129.47 (ArCH), 129.45 (ArCH), 128.3 (ArC), 128.2 (ArC), 128.1 (ArCH), 127.9 (ArCH), 121.7 (ArCH), 112.6 (ArCH), 80.4 (C_q), 70.8 (CH_2), 70.3 (CH_2), 68.1 (CH_2), 66.1 (CH_2), 65.7 (CH_2), 52.4 (CH_2), 49.7 (CH_2), 49.1 (CH_2), 28.5 (CH_3), 18.6 (CH_3), 10.84 (CH), 10.82 (CH) (four carbon signals obscured or overlapping). IR (KBr, cm^{-1}) 3431, 3145, 2944, 2890, 2866, 1721, 1695, 1505, 1461, 1267, 1252, 1129, 844. MS (FAB+) $m/z = 1758$ [$\text{M} - \text{PF}_6$]⁺. Anal. Calcd for $\text{C}_{103}\text{H}_{157}\text{F}_6\text{N}_2\text{O}_{14}\text{PSi}_4$: C 64.95, H 8.31, N 1.49. Found: C 65.24, H 8.12, N 1.16.

1a. Rotaxane **8a** (50.0 mg, 0.0263 mmol) was treated according to General Procedure B to provide the desired bis-hexafluorophosphate salt **1a** as an off-white solid (45.9 mg, 90%). Mp $118\text{--}120\text{ }^\circ\text{C}$. ^1H NMR (400 MHz, CDCl_3) δ_{H} (ppm) 8.20 (d, $J = 0.7\text{ Hz}$, 2 H), 8.19 (d, $J = 0.8\text{ Hz}$, 2 H), 7.86–7.81 (m, 2 H), 7.80–7.62 (br m, 6 H), 7.59–7.47 (br m, 4 H), 7.46–7.38 (m, 2 H), 7.28 (d, $J = 8.1\text{ Hz}$, 2 H), 7.22 (d, $J = 8.1\text{ Hz}$, 2 H), 6.77 (s, 8 H), 5.38 (s, 2 H), 5.31 (s, 2 H), 4.69–4.60 (m, 2 H), 4.49–4.41 (m, 2 H), 4.34 (br s, 2 H), 4.17–3.98 (overlapping m, 10 H), 3.82–3.65 (m, 8 H), 3.45–3.27 (8 H), 1.51–1.35 (m, 12 H), 1.07 (d, $J = 7.5\text{ Hz}$, 72 H). ^{13}C NMR (100 MHz, CDCl_3) δ_{C} (ppm) 167.3 (C=O), 167.1 (C=O), 147.6 (ArC), 147.3 (ArCH), 147.2 (ArCH), 138.6 (ArC), 138.0 (ArC), 136.7 (ArCH), 136.5 (ArCH), 134.4 (ArC), 134.3 (ArC), 133.3 (ArC), 131.6 (ArC), 131.2 (ArC), 131.1 (ArC), 131.0 (ArCH), 130.3 (ArCH), 129.4 (ArCH), 128.4 (ArCH), 128.2 (ArC), 128.1 (ArC), 127.8 (ArCH), 122.0 (ArCH), 113.2 (ArCH), 70.7 (CH_2), 70.3 (CH_2), 68.5 (CH_2), 65.8 (CH_2), 65.7 (CH_2), 52.6 (CH_2), 52.5 (CH_2), 52.3 (CH_2), 51.2 (CH_2), 18.6 (two overlapping CH_3 signals), 10.9 (two overlapping CH signals) (one ArCH signal obscured or overlapping). IR (KBr, cm^{-1}) 3421, 2944, 2889, 2866, 1721, 1506, 1457, 1267, 1252, 1130, 849. MS (FAB+) $m/z = 1658$ [$\text{M} - 2\text{PF}_6 - \text{H}$]⁺. Anal. Calcd for $\text{C}_{98}\text{H}_{150}\text{F}_{12}\text{N}_2\text{O}_{12}\text{P}_2\text{Si}_4$: C, 60.35; H, 7.75; N, 1.44. Found: C, 60.26; H, 8.15; N, 1.45.

3b. Diamine **2b** (0.865 g, 1.701 mmol) was treated according to General Procedure C. Purification by column chromatography (silica gel, $\text{CH}_2\text{Cl}_2/\text{acetone}$ [20:1 to 1:1]) provided the desired mono-Boc-protected product **3b** (0.550 g, 53%) and the di-Boc-protected product **9** (0.423 g, 35%) both as colorless oils. Compound **3b**: $R_f = 0.25$ (acetone/ CH_2Cl_2 [1:10]). ^1H NMR (400 MHz, CDCl_3) δ_{H} (ppm) 8.03–7.98 (m, 4 H), 7.58–7.52 (m, 4 H), 7.44 (d, $J = 8.2\text{ Hz}$, 2 H), 7.41 (d, $J = 8.1\text{ Hz}$, 2 H), 7.34–7.20 (br m, 4 H), 4.49 (br s, 2 H), 4.42 (br s, 2 H), 3.908 (s, 3 H), 3.905 (s, 3 H), 3.89 (s, 2 H), 3.84 (s, 2 H), 1.74 (s, 1 H), 1.50 (br s, 9 H). ^{13}C NMR (100 MHz, CDCl_3) δ_{C} (ppm) 167.0 (C=O), 166.9 (C=O), 155.9 (C=O), 145.7 (ArC), 143.5 (ArC), 140.1 (ArC), 139.6 (ArC), 139.3 (ArC), 136.7 (ArC), 129.9 (ArCH), 129.8 (ArCH), 129.2 (ArC), 128.9 (ArC), 128.6 (ArCH), 128.5 (ArC), 128.0 (ArC), 127.8 (ArC), 127.2 (ArC), 127.1 (ArC), 80.4 (C_q), 52.9 (CH_2), 52.8 (CH_2), 52.1 (CH_3), 52.0 (CH_3), 49.4 (CH_2), 49.1 (CH_2), 28.4 (CH_3). IR (KBr, cm^{-1}) 3418, 2976, 2950, 1720, 1693, 1279, 1163, 753. MS (FAB+) $m/z = 609$ [$\text{M} + \text{H}$]⁺. HRMS (FAB+) m/z calcd for $\text{C}_{37}\text{H}_{41}\text{N}_2\text{O}_6$ [$\text{M} + \text{H}$]⁺ 609.2965, found 609.2969. Compound **9**: $R_f = 0.81$ (acetone/ CH_2Cl_2 [1:10]). ^1H

NMR (400 MHz, CDCl₃) δ_{H} (ppm) 8.01 (d, *J* = 8.2 Hz, 4 H), 7.55 (d, *J* = 8.2 Hz, 4 H), 7.38–7.19 (br m, 8 H), 4.50 (br s, 4 H), 4.43 (br s, 4 H), 3.91 (s, 6 H), 1.50 (s, 18 H). ¹³C NMR (100 MHz, CDCl₃) δ_{C} (ppm) 166.8 (C=O), 155.9 (C=O), 143.5 (ArC), 139.9 (ArC), 136.9 (ArC), 129.9 (ArCH), 129.2 (ArC), 128.5 (ArCH), 128.0 (ArCH), 127.2 (ArCH), 80.4 (C_q), 52.0 (CH₃), 49.5 (CH₂), 49.1 (CH₂), 28.4 (CH₃). IR (KBr, cm⁻¹) 3437, 2974, 1715, 1695, 1284, 1164, 1130, 1107, 891, 750. MS (FAB+) *m/z* = 708 [M]⁺. HRMS (FAB+) *m/z* calcd for C₄₅H₄₈N₂O₈ [M]⁺ 708.3411, found 708.3426.

4b. Mono-Boc compound **3b** (0.550 g, 0.9035 mmol) was treated according to General Procedure D. Purification by column chromatography (silica gel, acetone/CH₂Cl₂ [1:20 to 3:1]) gave the desired diol **4b** as a colorless oil (0.447 g, 89%). *R_f* = 0.21 (acetone/CH₂Cl₂ [3:1]). ¹H NMR (400 MHz, CDCl₃) δ_{H} (ppm) 7.57–7.50 (m, 4 H), 7.36 (d, *J* = 8.1 Hz, 2 H), 7.32–7.28 (overlapping m, 2 H), 7.28 (s, 4 H), 7.28–7.14 (br overlapping m, 4 H), 4.62 (s, 2 H), 4.61 (s, 2 H), 4.45–4.30 (2 br overlapping s, 4 H), 3.78 (s, 2 H), 3.77 (s, 2 H), 2.52 (br s, 2 H), 1.49 (s, 9 H). One \times NH not observed. ¹³C NMR (100 MHz, CDCl₃) δ_{C} (ppm) 156.1 (C=O), 140.3 (ArC), 140.1 (ArC), 139.9 (ArC), 139.6 (ArC), 139.2 (ArC), 139.1 (ArC), 137.2 (ArC), 137.0 (ArC), 128.7 (ArCH), 128.4 (ArCH), 128.3 (ArCH), 127.8 (ArCH), 127.24 (ArCH), 127.19 (ArCH), 127.16 (ArCH), 127.1 (ArCH), 80.3 (C_q), 64.81 (CH₂), 64.75 (CH₂), 52.8 (CH₂), 52.7 (CH₂), 49.1 (CH₂), 48.9 (CH₂), 28.5 (CH₃). IR (KBr, cm⁻¹) 3297, 3024, 2975, 2863, 1690, 1678, 1412, 1162, 805. MS (FAB+) *m/z* = 553 [M + H]⁺. HRMS (FAB+) *m/z* calcd for C₃₅H₄₁N₂O₄ [M + H]⁺ 553.3066, found 553.3068.

5b. Compound **4b** (0.351 g, 0.6351 mmol) was treated according to General Procedure E to afford the desired hexafluorophosphate salt **5b** as a colorless foam (0.337 g, 76%), which was used in the next step without further purification.

8b. Hexafluorophosphate salt **5b** (70.0 mg, 0.100 mmol) was treated according to General Procedure A. The crude product was subjected twice to column chromatography (column 1: silica gel, CHCl₃/EtOAc [10:1 to 5:1]; column 2: silica gel, acetone/CH₂Cl₂ [1:20]) to give the desired rotaxane **8b** as a colorless foam (0.127 g, 64%). *R_f* = 0.28 (acetone/CH₂Cl₂ [1:20]). Mp 105–106 °C. ¹H NMR (400 MHz, CDCl₃) δ_{H} (ppm) 8.21 (d, *J* = 1.1 Hz, 2 H), 8.19 (d, *J* = 1.1 Hz, 2 H), 7.86–7.81 (m, 2 H), 7.72–7.60 (br m, 2 H), 7.49 (d, *J* = 8.2 Hz, 2 H), 7.47–7.40 (m, 4 H), 7.37 (d, *J* = 8.2 Hz, 2 H), 7.33–7.21 (overlapping m, 8 H), 6.85–6.71 (m, 8 H), 5.39 (s, 2 H), 5.30 (s, 2 H), 4.71–4.59 (m, 4 H), 4.45 (br s, 2 H), 4.39 (br s, 2 H), 4.16–4.03 (m, 8 H), 3.85–3.72 (m, 8 H), 3.56–3.44 (m, 8 H), 1.51 (s, 9 H), 1.43 (sept, *J* = 2.5 Hz, 12 H), 1.08 (d, *J* = 2.5 Hz, 36 H), 1.07 (d, *J* = 2.5 Hz, 36 H). ¹³C NMR (100 MHz, CDCl₃) δ_{C} (ppm) 167.3 (C=O), 167.0 (C=O), 156.0 (C=O), 147.5 (ArC), 147.2 (ArCH), 147.0 (ArCH), 141.6 (ArC), 138.9 (ArC), 138.8 (ArC), 137.7 (ArC), 136.54 (ArCH), 136.46 (ArCH), 135.6 (ArC), 134.3 (ArC), 134.1 (ArC), 131.4 (ArC), 130.5 (ArC), 129.7 (ArCH), 129.4 (ArCH), 128.4 (ArCH observed in DEPT), 128.3 (ArC), 128.1 (ArC), 128.0 (ArCH), 127.9 (ArCH), 127.6 (ArCH), 127.2 (ArCH), 127.1 (ArCH), 121.7 (ArCH), 112.7 (ArCH), 80.3 (C_q), 70.7 (CH₂), 70.3 (CH₂), 68.2 (CH₂), 66.1 (CH₂), 65.4 (CH₂), 52.3 (two overlapping CH₂ signals), 49.3 (CH₂), 48.9 (CH₂), 28.5 (CH₃), 18.5 (two overlapping CH₃ signals), 10.79 (CH), 10.77 (CH) (one carbon signal obscured or overlapping). IR (KBr, cm⁻¹) 3437, 2944, 2866, 1721, 1696, 1505, 1459, 1267, 1129, 844. MS (FAB+) *m/z* = 1835 [M - PF₆]⁺. Anal. Calcd for C₁₀₉H₁₆₁F₆N₂O₁₄PSi₄: C, 66.09; H, 8.19; N, 1.41. Found: C, 66.37; H, 8.18; N, 1.41.

1b. Rotaxane **8b** (0.121 g, 0.0611 mmol) was treated according to General Procedure B to provide the desired bis-hexafluorophosphate salt **1b** as an off-white foam (0.117 g, 94%). Mp 131–132 °C. ¹H NMR (400 MHz, CDCl₃) δ_{H} (ppm) 8.21–8.16 (m, 4 H), 7.86–7.81 (m, 2 H), 7.70–7.56 (overlapping br m, 2 H), 7.60 (d, *J* = 8.2 Hz, 2 H), 7.54 (d, *J* = 8.3 Hz, 2 H), 7.51–7.44 (m, 4 H), 7.37–7.24 (m, 8 H), 6.83–6.68 (m, 8 H), 5.34 (s, 2 H), 5.29 (s, 2 H), 4.71–4.57 (m, 4 H), 4.37 (s, 2 H), 4.26 (s, 2 H), 4.15–4.00 (m, 8 H), 3.84–3.70 (m, 8 H), 3.56–3.40 (m, 8 H), 1.50–1.34 (m, 12 H), 1.08 (d, *J* = 1.0 Hz, 36 H), 1.06 (d, *J* = 1.0 Hz, 36 H). ¹³C NMR (100 MHz, CDCl₃) δ_{C} (ppm) 167.3 (C=O), 167.2 (C=O), 147.5 (ArC), 147.3 (ArCH),

147.2 (ArCH), 141.3 (ArC), 140.9 (ArC), 138.6 (ArC), 137.9 (ArC), 136.6 (ArCH), 136.5 (ArCH), 134.4 (ArC), 134.3 (ArC), 131.6 (ArC), 131.0 (ArC), 130.8 (ArCH), 130.7 (ArCH), 129.8 (ArCH), 129.43 (ArCH), 129.35 (ArC), 129.1 (ArC), 128.5 (ArCH), 128.2 (ArC), 128.1 (ArC), 129.0 (ArCH), 127.9 (ArCH), 127.3 (ArCH), 121.9 (ArCH), 112.8 (ArCH), 70.8 (CH₂), 70.4 (CH₂), 68.2 (CH₂), 65.8 (two overlapping CH₂ signals observed in HMQC), 52.44 (CH₂), 52.39 (CH₂), 51.9 (CH₂), 51.5 (CH₂), 18.6 (two overlapping CH signals), 10.9 (two overlapping CH₃ signals). IR (KBr, cm⁻¹) 3437, 2943, 2866, 1721, 1505, 1459, 1267, 1130, 841, 559. MS (FAB+) *m/z* = 1734 [M - 2PF₆ - H]⁺. Anal. Calcd for C₁₀₄H₁₅₄F₁₂N₂O₁₂P₂Si₄: C, 61.64; H, 7.66; N, 1.38. Found: C, 61.25; H, 7.70; N, 1.41.

3c. Diamine **2c** (0.142 g, 0.242 mmol) was treated according to General Procedure C. Purification by column chromatography (silica gel, EtOAc/hexane [4:1 to neat EtOAc]) and evaporation of appropriate fractions gave the desired mono-Boc-protected product **3c** (85.8 mg, 52%) as a colorless oil and the di-Boc-protected product **10** (53.3 mg, 28%) as a colorless solid. Compound **3c**: *R_f* = 0.56 (EtOAc/hexane [4:1]). ¹H NMR (400 MHz, CDCl₃) δ_{H} (ppm) 8.05–7.98 (m, 4 H), 7.87 (s, 4 H), 7.64–7.58 (m, 4 H), 7.47–7.41 (m, 4 H), 7.29 (br s, 4 H), 4.56–4.35 (2 overlapping br s, 4 H), 3.93–3.92 (2 overlapping s, 6 H), 3.91 (s, 2 H), 3.87 (s, 2 H), 1.73 (br s, 1 H), 1.51 (s, 9 H). ¹³C NMR (100 MHz, CDCl₃) δ_{C} (ppm) 167.1, 166.9, 156.0, 145.8, 143.6, 139.94, 139.87, 139.6, 139.5, 139.4, 136.9, 129.9, 129.8, 129.3, 129.0, 128.7, 128.6, 128.1, 127.8, 127.5, 127.4, 127.2, 127.1, 80.5, 52.93, 52.87, 52.1, 52.1, 49.6, 49.2, 28.5. IR (KBr, cm⁻¹) 3422, 3027, 2976, 2951, 2840, 1721, 1691, 1612, 1280, 1164, 1109, 805, 755. MS (FAB+) *m/z* = 685 [M + H]⁺. HRMS (FAB+) *m/z* calcd for C₄₃H₄₅N₂O₆ [M + H]⁺ 685.3278, found 685.3260. Compound **10**: *R_f* = 0.92 (EtOAc/hexane [4:1]). Mp 186–187 °C. ¹H NMR (400 MHz, CDCl₃) δ_{H} (ppm) 8.01 (d, *J* = 8.3 Hz, 4 H), 7.68 (s, 4 H), 7.61 (d, *J* = 8.2 Hz, 4 H), 7.30 (br s, 8 H), 4.57–4.35 (2 overlapping br s, 8 H), 3.92 (s, 6 H), 1.51 (s, 18 H). ¹³C NMR (100 MHz, CDCl₃) δ_{C} (ppm) 166.9, 156.0, 143.6, 139.9, 139.8, 137.0, 130.0, 129.3, 128.6, 128.0, 127.5, 127.3, 80.5, 52.1, 49.6, 49.3, 28.5. IR (KBr, cm⁻¹) 3430, 2978, 1693, 1612, 1466, 1281, 1250, 1131, 964, 761, 491. MS (FAB+) *m/z* = 784 [M]⁺. HRMS (FAB+) *m/z* calcd for C₄₈H₅₂N₂O₈ [M]⁺ 784.3724, found 784.3752.

4c. Mono-Boc compound **3c** (0.402 g, 0.587 mmol) was treated according to General Procedure D to give the desired diol **4c** as a colorless foam (0.337 g, 91%). *R_f* = 0.31 (CHCl₃/CH₃OH). Mp 55–56 °C. ¹H NMR (400 MHz, CDCl₃) δ_{H} (ppm) 7.68 (s, 4 H), 7.65–7.58 (m, 4 H), 7.42 (d, *J* = 8.1 Hz, 2 H), 7.38–7.18 (br overlapping m, 8 H), 7.34 (s, 2 H), 4.67 (s, 2 H), 4.66 (s, 2 H), 4.52–4.33 (2 br overlapping s, 4 H), 3.83 (s, 2 H), 3.82 (s, 2 H), 1.53 (s, 9 H). One \times NH, 2 \times OH not observed. ¹³C NMR (100 MHz, CDCl₃) δ_{C} (ppm) 156.2, 140.3, 140.1, 139.9, 139.8, 139.5, 139.3, 139.2, 137.2, 128.8, 128.5, 128.3, 128.1, 127.7, 127.48, 127.46, 127.3, 127.2, 127.1, 80.4, 65.00, 64.95, 52.9, 52.7, 49.2, 49.0, 28.6 (one carbon signal obscured or overlapping). IR (KBr, cm⁻¹) 3382, 3026, 2975, 2927, 2868, 1688, 1492, 1459, 1407, 1365, 1246, 1162, 804. MS (FAB+) *m/z* = 629 [M + H]⁺. HRMS (FAB+) *m/z* calcd for C₄₁H₄₅N₂O₄ [M + H]⁺ 629.3379, found 629.3389.

5c. Compound **4c** (0.335 g, 0.533 mmol) was treated according to General Procedure E to afford the desired hexafluorophosphate salt **5c** as a colorless foam (0.412 g, quant), which was used in the next step without further purification.

8c. Hexafluorophosphate salt **5c** (87.9 mg, 0.0113 mmol) was treated according to General Procedure A. The crude product was subjected twice to column chromatography (column 1: silica gel, CHCl₃/EtOAc [6:1 then CHCl₃/CH₃OH [20:1]; column 2: silica gel, acetone/CH₂Cl₂ [1:20]) to give the desired rotaxane **8c** as a colorless foam (0.159 g, 68%). *R_f* = 0.28 (acetone/CH₂Cl₂ [1:20]), 0.34 (CHCl₃/CH₃OH [20:1]). Mp 113–115 °C. ¹H NMR (400 MHz, CDCl₃) δ_{H} (ppm) 8.21 (d, *J* = 1.0 Hz, 2 H), 8.19 (d, *J* = 1.0 Hz, 2 H), 7.90–7.84 (m, 2 H), 7.73–7.58 (overlapping m, 8 H), 7.50 (d, *J* = 5.0 Hz, 2 H), 7.44 (d, *J* = 8.0 Hz, 2 H), 7.39 (d, *J* = 8.2 Hz, 2 H), 7.36–7.23 (overlapping m, 8 H), 6.85–6.72 (m, 8 H), 5.39 (s, 2 H), 5.30 (s, 2 H), 4.72–4.60 (br m, 4 H), 4.53–4.35 (2 overlapping br s, 4 H), 4.17–4.04 (m, 8 H), 3.86–3.73 (m, 8 H), 3.51 (s, 8 H), 1.51 (s, 9

H), 1.44 (sept, $J = 3.1$ Hz, 12 H), 1.09 (d, $J = 3.1$ Hz, 36 H), 1.07 (d, $J = 3.1$ Hz, 36 H). ^{13}C NMR (100 MHz, CDCl_3) δ_{C} (ppm) 167.3, 167.1, 156.1, 147.5, 147.2, 147.1, 136.6, 136.5, 129.5, 128.1, 127.9, 127.5, 127.3, 127.1, 121.8, 112.7, 80.3, 70.8, 70.3, 68.2, 66.2, 65.7, 52.4, 49.2, 49.0, 28.6, 18.6, 10.9, 10.8 (four carbon signals obscured or overlapping). IR (KBr, cm^{-1}) 3438, 3150, 2944, 2866, 1721, 1697, 1505, 1460, 1266, 1129, 844. MS (FAB+) $m/z = 1911$ [$\text{M} - \text{PF}_6$] $^+$. Anal. Calcd for $\text{C}_{115}\text{H}_{165}\text{F}_6\text{N}_2\text{O}_{14}\text{P}_5\text{Si}_4$: C, 67.15; H, 8.09; N, 1.36. Found: C, 66.93; H, 8.33; N, 1.36.

1c. Rotaxane **8c** (0.159 g, 0.0773 mmol) was treated according to General Procedure B to provide the desired bis-hexafluorophosphate salt **1c** as an off-white solid (0.149 g, 91%). Mp 134–136 °C. ^1H NMR (400 MHz, CDCl_3) δ_{H} (ppm) 8.19 (d, $J = 1.1$ Hz, 2 H), 8.18 (d, $J = 1.1$ Hz, 2 H), 7.85–7.81 (m, 2 H), 7.70–7.61 (br overlapping m, 2 H), 7.59 (d, $J = 8.2$ Hz, 2 H), 7.53–7.41 (overlapping m, 12 H), 7.38–7.34 (m, 2 H), 7.32–7.22 (m, 4 H), 6.90–6.80 (overlapping br m, 2 H), 6.80–6.69 (m, 8 H), 5.34 (s, 2 H), 5.28 (s, 2 H), 4.73–4.55 (m, 4 H), 4.37 (br s, 2 H), 4.24 (br s, 2 H), 4.16–3.97 (m, 8 H), 3.84–3.66 (m, 8 H), 3.59–3.39 (m, 8 H), 1.47–1.35 (m, 12 H), 1.07 (d, $J = 3.3$ Hz, 36 H), 1.05 (d, $J = 3.3$ Hz, 36 H). ^{13}C NMR (100 MHz, CDCl_3) δ_{C} (ppm) 167.3 (C=O), 167.2 (C=O), 147.5 (ArC), 147.3 (ArCH), 147.2 (ArCH), 142.0 (ArC), 141.2 (ArC), 139.20 (ArC), 139.17 (ArC), 138.6 (ArC), 137.8 (ArC), 136.62 (ArCH), 136.55 (ArCH), 134.4 (ArC), 134.3 (ArC), 131.6 (ArC), 130.8 (ArCH), 130.7 (ArCH), 129.9 (ArCH), 129.5 (ArCH), 129.3 (ArC), 128.7 (ArC), 128.5 (ArCH), 128.2 (ArC), 128.1 (ArC), 127.9 (ArCH), 127.8 (ArCH), 127.5 (ArCH), 127.2 (ArCH), 121.8 (ArCH), 112.8 (ArCH), 70.8 (CH_2), 70.4 (CH_2), 68.20 (CH_2), 65.8 (two overlapping CH_2 signals observed in HMQC), 52.5 (CH_2), 52.4 (CH_2), 51.9 (CH_2), 51.6 (CH_2), 18.6 (two overlapping CH_3 signals), 10.9 (two overlapping CH signals) (one ArC, one ArCH signal). IR (KBr, cm^{-1}) 3422, 3148, 2944, 2866, 1721, 1505, 1459, 1267, 1130, 846, 558. MS (FAB+) $m/z = 1810$ [$\text{M} - 2\text{PF}_6 - \text{H}$] $^+$. Anal. Calcd for $\text{C}_{110}\text{H}_{158}\text{F}_{12}\text{N}_2\text{O}_{12}\text{P}_2\text{Si}_4$: C, 62.83; H, 7.57; N, 1.33. Found: C, 62.90; H, 7.86; N, 1.34.

3d. Diamine **2d** (0.500 g, 0.757 mmol) was treated according to General Procedure C. Purification by column chromatography (silica gel, acetone/ CH_2Cl_2 [1:20 to 10:1]) provided the desired mono-Boc-protected product **3d** (0.261 g, 45%) and the di-Boc-protected product **11** (0.150 g, 23%), both as pale-yellow solids. Compound **3d**: $R_f = 0.52$ (acetone/ CH_2Cl_2 [1:10]), 0.27 (acetone/ CH_2Cl_2 [1:20]). Mp 131–133 °C. ^1H NMR (400 MHz, CDCl_3) δ_{H} (ppm) 8.04–7.98 (m, 4 H), 7.74–7.66 (m, 8 H), 7.64–7.58 (m, 4 H), 7.47–7.40 (m, 4 H), 7.35–7.24 (br m, 4 H), 4.50 (br s, 2 H), 4.43 (br s, 2 H), 3.91 (s, 6 H), 3.90 (s, 2 H), 3.85 (s, 2 H), 1.72 (s, 1 H), 1.50 (s, 9 H). ^{13}C NMR (100 MHz, CDCl_3) δ_{C} (ppm) 167.0 (C=O), 166.9 (C=O), 156.0 (C=O), 145.7 (ArC), 143.5 (ArC), 139.9 (ArC), 139.8 (ArC), 139.7 (ArC), 139.6 (ArC), 139.5 (ArC), 139.3 (ArC), 136.9 (ArC), 129.9 (ArCH), 129.8 (ArCH), 129.2 (ArC), 128.9 (ArC), 128.8 (ArCH), 128.7 (ArCH), 128.5 (ArCH), 128.0 (ArCH), 127.8 (ArCH), 127.39 (ArCH), 127.36 (ArCH), 127.2 (ArCH), 127.1 (ArCH), 80.5 (C_q), 52.9 (CH_2), 52.8 (CH_2), 52.1 (CH_3), 52.0 (CH_3), 49.5 (CH_2), 49.1 (CH_2), 28.4 (CH_3) (two carbon signals obscured or overlapping). IR (KBr, cm^{-1}) 3422, 2975, 2841, 1721, 1692, 1611, 1280, 1160, 1108, 805, 756. MS (FAB+) $m/z = 761$ [$\text{M} + \text{H}$] $^+$. HRMS (FAB+) m/z calcd for $\text{C}_{49}\text{H}_{49}\text{N}_2\text{O}_6$ [$\text{M} + \text{H}$] $^+$ 761.3591, found 761.3589. Compound **11**: $R_f = 0.50$ (acetone/ CH_2Cl_2 [1:60]), 0.88 (acetone/ CH_2Cl_2 [1:20]). Mp 197–198 °C. ^1H NMR (400 MHz, CDCl_3) δ_{H} (ppm) 8.01 (d, $J = 8.2$ Hz, 4 H), 7.70 (app. q, $J = 8.4$ Hz, 8 H), 7.61 (d, $J = 8.1$ Hz, 4 H), 7.39–7.18 (br m, 8 H), 4.51 (br s, 4 H), 4.43 (br s, 4 H), 3.90 (s, 6 H), 1.50 (s, 18 H). ^{13}C NMR (100 MHz, CDCl_3) δ_{C} (ppm) 166.9 (C=O), 155.9 (C=O), 143.5 (ArC), 143.4 (ArC), 139.8 (ArC), 139.6 (ArC), 136.9 (ArC), 129.9 (ArCH), 129.2 (ArC), 128.5 (ArCH), 127.9 (ArCH), 127.44 (ArCH), 127.37 (ArCH), 127.2 (ArCH), 80.4 (C_q), 52.04 (CH_3), 49.50 (CH_2), 49.12 (CH_2), 28.43 (CH_3). IR (KBr, cm^{-1}) 3422, 3025, 2978, 2929, 1714, 1699, 1613, 1488, 1397, 1280, 1249, 1165, 1111, 801, 752. MS (FAB+) $m/z = 860$ [M] $^+$. HRMS (FAB+) m/z calcd for $\text{C}_{54}\text{H}_{56}\text{N}_2\text{O}_8$ [M] $^+$ 860.4037, found 860.4016.

4d. Mono-Boc compound **3d** (0.250 g, 0.329 mmol) was treated according to General Procedure D. Purification by column chromatography (silica gel, acetone/ CH_2Cl_2 [1:10 to 1:1]) afforded the desired diol **4d** as an off-white solid (0.167 g, 72%). $R_f = 0.27$ (acetone/ CH_2Cl_2 [1:1]). Mp 117–119 °C. ^1H NMR (400 MHz, $\text{CDCl}_3/\text{CD}_3\text{OD}$ [10:1]) δ_{H} (ppm) 7.75–7.67 (m, 8 H), 7.64 (d, $J = 8.1$ Hz, 2 H), 7.62 (d, $J = 8.1$ Hz, 2 H), 7.40 (d, $J = 8.2$ Hz, 2 H), 7.38–7.30 (m, 6 H), 7.30–7.16 (br m, 4 H), 4.642 (s, 2 H), 4.637 (s, 2 H), 4.45 (br s, 2 H), 4.39 (br s, 4 H), 3.82 (s, 2 H), 3.81 (s, 2 H), 1.52 (s, 9 H). ^{13}C NMR (100 MHz, CDCl_3) δ_{C} (ppm) 156.3 (C=O), 140.3 (ArC), 140.2 (ArC), 139.7 (ArC), 139.6 (ArC), 139.5 (ArC), 139.43 (ArC), 139.40 (ArC), 138.2 (ArC), 138.1 (ArC), 136.9 (ArC), 136.7 (ArC), 136.6 (ArC), 128.8 (ArCH), 128.3 (ArCH), 127.8 (ArCH), 127.4 (ArCH), 127.3 (ArCH), 127.2 (ArCH), 127.10 (ArCH), 127.07 (ArCH), 127.02 (ArCH), 126.98 (ArCH), 80.5 (C_q), 64.13 (CH_2), 64.09 (CH_2), 52.4 (CH_2), 52.2 (CH_2), 49.1 (CH_2 observed in DEPT), 48.8 (CH_2 observed in DEPT), 28.2 (CH_3) (two carbon signals obscured or overlapping). IR (KBr, cm^{-1}) 3421, 2931, 1683, 1489, 1244, 1160, 805. MS (FAB+) $m/z = 705$ [$\text{M} + \text{H}$] $^+$. HRMS (FAB+) m/z calcd for $\text{C}_{47}\text{H}_{49}\text{N}_2\text{O}_4$ [$\text{M} + \text{H}$] $^+$ 705.3692, found 705.3696.

5d. Compound **4d** was treated according to General Procedure E to afford the desired hexafluorophosphate salt **5d** as a pale yellow solid (0.202 g, quant), which was used in the next step without further purification.

8d. Hexafluorophosphate salt **5d** (87.9 mg, 0.0113 mmol) was treated according to General Procedure A. The crude product was subjected twice to column chromatography (column 1: silica gel, $\text{CHCl}_3/\text{EtOAc}$ [10:1 to 5:1]; column 2: silica gel, acetone/ CH_2Cl_2 [1:20]) to give the desired rotaxane **8d** as a colorless solid (0.109 g, 72%). $R_f = 0.43$ (acetone/ CH_2Cl_2 [20:1]). Mp 119–121 °C. ^1H NMR (400 MHz, CDCl_3) δ_{H} (ppm) 8.20 (d, $J = 8.3$ Hz, 4 H), 7.85–7.81 (m, 2 H), 7.75–7.58 (m, 12 H), 7.50 (d, $J = 8.3$ Hz, 2 H), 7.43 (d, $J = 8.1$ Hz, 2 H), 7.39 (d, $J = 8.2$ Hz, 2 H), 7.35–7.20 (m, 8 H), 6.85–6.70 (m, 8 H), 5.39 (s, 2 H), 5.29 (s, 2 H), 4.73–4.59 (m, 4 H), 4.47 (br s, 2 H), 4.40 (br s, 2 H), 4.18–4.02 (m, 8 H), 3.86–3.71 (m, 8 H), 3.59–3.44 (m, 8 H), 1.51 (s, 9 H), 1.48–1.36 (m, 12 H), 1.08 (d, $J = 4.3$ Hz, 36 H), 1.06 (d, $J = 4.2$ Hz, 36 H). ^{13}C NMR (100 MHz, CDCl_3) δ_{C} (ppm) 167.4 (C=O), 167.2 (C=O), 156.2 (C=O), 147.5 (ArC), 147.3 (ArCH), 147.1 (ArCH), 141.5 (ArC), 140.1 (ArC), 140.0 (ArC), 139.8 (ArC), 139.5 (ArC), 138.9 (ArC), 138.0 (ArC), 137.9 (ArC), 137.3 (ArC), 136.7 (ArCH), 136.6 (ArCH), 135.7 (ArC), 134.4 (ArCH), 134.2 (ArCH), 131.5 (ArC), 130.7 (ArC), 129.9 (ArCH), 129.5 (ArCH), 128.6 (ArCH), 128.4 (ArC), 128.2 (ArC), 128.1 (ArCH), 128.0 (ArCH), 127.6 (ArCH), 127.53 (ArCH), 127.51 (ArCH), 127.3 (ArCH), 127.2 (ArCH), 121.8 (ArCH), 112.8 (ArCH), 80.4 (C_q), 70.8 (CH_2), 70.4 (CH_2), 68.2 (CH_2), 66.2 (CH_2), 65.8 (CH_2), 52.5 (two overlapping CH_2 signals observed in HMQC), 49.3 (CH_2), 49.0 (CH_2), 28.6 (CH_3), 18.7 (two overlapping CH signals), 10.90 (CH), 10.88 (CH) (two ArC signals obscured or overlapping). IR (KBr, cm^{-1}) 3447, 3148, 2943, 2866, 1721, 1697, 1505, 1459, 1251, 1129, 844. MS (FAB+) $m/z = 1986$ [$\text{M} - \text{PF}_6$] $^+$. Anal. Calcd for $\text{C}_{121}\text{H}_{169}\text{F}_6\text{N}_2\text{O}_{14}\text{PSi}_4$: C, 68.14; H, 7.99; N, 1.31. Found: C, 68.01; H, 8.00; N, 1.32.

1d. Rotaxane **8d** (0.121 g, 0.0567 mmol) was treated according to General Procedure B to provide the desired bis-hexafluorophosphate salt **1d** as an off-white solid (0.114 g, 92%). Mp 146–149 °C. ^1H NMR (400 MHz, CDCl_3) δ_{H} (ppm) 8.39–8.23 (br s, 2 H), 8.20 (d, $J = 0.9$ Hz, 2 H), 8.18 (d, $J = 0.9$ Hz, 2 H), 7.85–7.80 (m, 2 H), 7.70–7.42 (m, 20 H), 7.37 (d, $J = 8.3$ Hz, 2 H), 7.29 (d, $J = 8.3$ Hz, 2 H), 7.25 (d, $J = 8.3$ Hz, 2 H), 6.82–6.68 (m, 8 H), 5.32 (s, 2 H), 5.28 (s, 2 H), 4.72–4.55 (br m, 4 H), 4.23–4.13 (br m, 2 H), 4.13–4.08 (overlapping br m, 2 H), 4.11–3.99 (m, 8 H), 3.83–3.69 (m, 8 H), 3.56–3.41 (m, 8 H), 1.50–1.33 (m, 12 H), 1.07 (d, $J = 3.3$ Hz, 36 H), 1.05 (d, $J = 3.3$ Hz, 36 H). ^{13}C NMR (100 MHz, CDCl_3) δ_{C} (ppm) 167.3 (C=O), 167.2 (C=O), 147.5 (ArC), 147.3 (ArCH), 147.2 (ArCH), 141.8 (ArC), 141.5 (ArC), 134.0 (ArC), 139.7 (ArC), 139.2 (ArC), 138.8 (ArC), 138.2 (ArC), 137.9 (ArC), 136.7 (ArCH), 136.6 (ArCH), 134.4 (ArC), 134.3 (ArC), 131.6 (ArC), 130.8 (ArCH), 130.64 (ArC), 130.62 (ArCH), 129.88 (ArCH), 129.86 (ArC), 129.5

(ArCH), 129.2 (ArC), 128.4 (ArCH), 128.2 (ArC), 127.9 (ArCH), 127.7 (ArCH), 127.5 (ArCH), 127.5 (ArCH), 127.4 (ArCH), 127.2 (ArCH), 121.9 (ArCH), 112.8 (ArCH), 70.8 (CH₂), 70.4 (CH₂), 68.2 (CH₂), 65.84 (CH₂), 65.77 (CH₂), 52.5 (CH₂), 52.4 (CH₂), 50.6 (CH₂), 50.4 (CH₂), 18.7 (two overlapping CH₃ signals), 10.9 (two overlapping CH signals) (one ArC signal, one ArCH signal obscured or overlapping). IR (KBr, cm⁻¹) 3421, 3150, 2944, 2866, 1721, 1505, 1459, 1267, 1129, 882. MS (FAB+) *m/z* = 1886 [M - 2PF₆ - H]⁺. Anal. Calcd for C₁₁₆H₁₆₂F₁₂N₂O₁₂P₂Si₄: C, 63.95; H, 7.49; N, 1.29. Found: C, 63.85; H, 7.30; N, 1.30.

■ ASSOCIATED CONTENT

● Supporting Information

Synthesis of axle precursors **2a–2d**, characterization, spectral data of all new compounds, additional experimental results. This material is available free of charge via the Internet at <http://pubs.acs.org>.

■ AUTHOR INFORMATION

Corresponding Author

hirose@chem.es.osaka-u.ac.jp

Notes

The authors declare no competing financial interest.

■ ACKNOWLEDGMENTS

This work was supported by a Grant-in-Aid for Scientific Research, Platform for Drug Discovery, Informatics, Structural Life Science from the Ministry of Education, Culture, Sports, Science, Technology, Japan (21350076, 24651139). P.G.Y. gratefully acknowledges the JSPS for his fellowship (P11737).

■ REFERENCES

- (1) (a) Fahrenbach, A. C.; Warren, S. C.; Incorvati, J. T.; Avestro, A.-J.; Barnes, J. C.; Stoddart, J. F.; Grzybowski, B. A. *Adv. Mater.* **2013**, *25*, 331–348. (b) Coskun, A.; Spruell, J. M.; Barin, G.; Dichtel, W. R.; Flood, A. H.; Botros, Y. Y.; Stoddart, J. F. *Chem. Soc. Rev.* **2012**, *41*, 4827–4859. (c) Balzani, V.; Credi, A.; Venturi, M. *Chem. Soc. Rev.* **2009**, *38*, 1542–1550. (d) Saha, S.; Stoddart, J. F. *Chem. Soc. Rev.* **2007**, *36*, 77–92. (e) Kay, E. R.; Leigh, D. A.; Zerbetto, F. *Angew. Chem., Int. Ed.* **2007**, *46*, 72–191. (f) Browne, W. R.; Feringa, B. L. *Nat. Nanotechnol.* **2006**, *1*, 25–35. (g) Altieri, A.; Gatti, F. G.; Kay, E. R.; Leigh, D. A.; Martel, D.; Paolucci, F.; Slawin, A. M. Z.; Wong, J. K. Y. *J. Am. Chem. Soc.* **2003**, *125*, 8644–8654. (h) Balzani, V.; Credi, A.; Raymo, F. M.; Stoddart, J. F. *Angew. Chem., Int. Ed.* **2000**, *39*, 3348–3391.
- (2) (a) Li, H.; Zhu, Z.; Fahrenbach, A. C.; Savoie, B. M.; Ke, C.; Barnes, J. C.; Lei, J.; Zhao, Y.-L.; Lilley, L. M.; Marks, T. J.; Ratner, M. A.; Stoddart, J. F. *J. Am. Chem. Soc.* **2013**, *135*, 456–467. (b) Pathem, B. K.; Claridge, S. A.; Zheng, Y. B.; Weiss, P. S.; Johnson, M. A.; Martinez, T. J. *Ann. Rev. Phys. Chem.* **2013**, *64*, 605–630. (c) Silvi, S.; Venturi, M.; Credi, A. *Chem. Commun.* **2011**, *47*, 2483–2489.
- (3) Anelli, P. L.; Spencer, N.; Stoddart, J. F. *J. Am. Chem. Soc.* **1991**, *113*, 5131–5133.
- (4) (a) Lane, A. S.; Leigh, D. A.; Murphy, A. J. *Am. Chem. Soc.* **1997**, *119*, 11092–11093. (b) Bissell, R. A.; Cordova, E.; Kaifer, A. E.; Stoddart, J. F. *Nature* **1994**, *369*, 133–137.
- (5) Moonen, N. N. P.; Flood, A. H.; Fernandez, J. M.; Stoddart, J. F. *Top. Curr. Chem.* **2005**, *262*, 99–132.
- (6) (a) Baggerman, J.; Haraszkiwicz, N.; Wiering, P. G.; Fioravanti, G.; Marcaccio, M.; Paolucci, F.; Kay, E. R.; Leigh, D. A.; Brouwer, A. M. *Chem.—Eur. J.* **2013**, *19*, 5566–5577. (b) Gunbas, D. D.; Brouwer, A. M. *J. Org. Chem.* **2012**, *77*, 5724–5735. (c) Li, H.; Zhao, Y.-L.; Fahrenbach, A. C.; Kim, S.-Y.; Paxton, W. F.; Stoddart, J. F. *Org. Biomol. Chem.* **2011**, *9*, 2240–2250. (d) Hmadeh, M.; Fahrenbach, A. C.; Basu, S.; Trabolsi, A.; Benitez, D.; Li, H.; Albrecht-Gary, A.-M.; Elhabiri, M.; Stoddart, J. F. *Chem.—Eur. J.* **2011**, *17*, 6076–6087.

- (e) Yoon, I.; Benitez, D.; Zhao, Y. L.; Miljanic, O. S.; Kim, S. Y.; Tkatchouk, E.; Leung, K. C. F.; Khan, S. I.; Goddard, W. A.; Stoddart, J. F. *Chem.—Eur. J.* **2009**, *15*, 1115–1122. (f) Nygaard, S.; Leung, K. C. F.; Aprahamian, I.; Ikeda, T.; Saha, S.; Laursen, B. W.; Kim, S.-Y.; Hansen, S. W.; Stein, P. C.; Flood, A. H.; Stoddart, J. F.; Jeppesen, J. O. *J. Am. Chem. Soc.* **2007**, *129*, 960–970. (g) Jeppesen, J. O.; Nygaard, S.; Vignon, S. A.; Stoddart, J. F. *Eur. J. Org. Chem.* **2005**, 196–220. (h) Garaudee, S.; Silvi, S.; Venturi, M.; Credi, A.; Flood, A. H.; Stoddart, J. F. *ChemPhysChem* **2005**, *6*, 2145–2152. (i) Kang, S. S.; Vignon, S. A.; Tseng, H. R.; Stoddart, J. F. *Chem.—Eur. J.* **2004**, *10*, 2555–2564. (j) Jeppesen, J. O.; Vignon, S. A.; Stoddart, J. F. *Chem.—Eur. J.* **2003**, *9*, 4611–4625.

(7) (a) Zazza, C.; Mancini, G.; Brancato, G.; Sanna, N.; Barone, V. *Comput. Theor. Chem.* **2012**, *985*, 53–61. (b) Zhang, K.-D.; Zhao, X.; Wang, G.-T.; Liu, Y.; Zhang, Y.; Lu, H.-J.; Jiang, X.-K.; Li, Z.-T. *Tetrahedron* **2012**, *68*, 4517–4527. (c) Kim, H.; Goddard, W. A., III; Jang, S. S.; Dichtel, W. R.; Heath, J. R.; Stoddart, J. F. *J. Phys. Chem. A* **2009**, *113*, 2136–2143. (d) Phoa, K.; Neaton, J. B.; Subramanian, V. *Nano Lett.* **2009**, *9*, 3225–3229. (e) Jang, S. S.; Jang, Y. H.; Kim, Y. H.; Goddard, W. A.; Choi, J. W.; Heath, J. R.; Laursen, B. W.; Flood, A. H.; Stoddart, J. F.; Norgaard, K.; Bjornholm, T. *J. Am. Chem. Soc.* **2005**, *127*, 14804–14816.

(8) Estimated for **1**¹ and **1**⁴ by molecular mechanics using the OPLS2005 force field by MacroModel.

(9) (a) Hirose, K. *J. Incl. Phenom. Macrocycl. Chem.* **2010**, *68*, 1–24. (b) Hirose, K.; Ishibashi, K.; Shiba, Y.; Doi, Y.; Tobe, Y. *Chem.—Eur. J.* **2008**, *14*, 5803–5811. (c) Hirose, K.; Shiba, Y.; Ishibashi, K.; Doi, Y.; Tobe, Y. *Chem.—Eur. J.* **2008**, *14*, 3427–3433. (d) Hirose, K.; Shiba, Y.; Ishibashi, K.; Doi, Y.; Tobe, Y. *Chem.—Eur. J.* **2008**, *14*, 981–986. (e) Hirose, K.; Ishibashi, K.; Shiba, Y.; Doi, Y.; Tobe, Y. *Chem. Lett.* **2007**, *36*, 810–811.

(10) Cao, J. G.; Fyfe, M. C. T.; Stoddart, J. F.; Cousins, G. R. L.; Glink, P. T. *J. Org. Chem.* **2000**, *65*, 1937–1946.

(11) Kawasaki, H.; Kihara, N.; Takata, T. *Chem. Lett.* **1999**, 1015–1016.

(12) (a) Zhu, K.; Vukotic, V. N.; Noujeim, N.; Loeb, S. J. *Chem. Sci.* **2012**, *3*, 3265–3271. (b) Zhu, K.; Vukotic, V. N.; Loeb, S. J. *Angew. Chem., Int. Ed.* **2012**, *51*, 2168–2172.

(13) Ashton, P. R.; Chrystal, E. J. T.; Glink, P. T.; Menzer, S.; Schiavo, C.; Spencer, N.; Stoddart, J. F.; Tasker, P. A.; White, A. J. P.; Williams, D. J. *Chem.—Eur. J.* **1996**, *2*, 709–728.

(14) (a) Oki, M. *Applications of Dynamic NMR Spectroscopy to Organic Chemistry*; VCH: Deerfield Beach, 1985; Vol. 4. (b) Pople, J. A.; Schneider, W. G.; Bernstein, H. J. *High-Resolution Nuclear Magnetic Resonance*; McGraw-Hill: New York, 1959.

(15) Gutmann, V. *Electrochim. Acta* **1976**, *21*, 661–670.

(16) Jeffrey, G. A. *An Introduction to Hydrogen Bonding*; Oxford University Press: New York, 1997; p 303.

(17) (a) Bartoli, S.; Roelens, S. *J. Am. Chem. Soc.* **1999**, *121*, 11908–11909. (b) Bartoli, S.; Roelens, S. *J. Am. Chem. Soc.* **2002**, *124*, 8307–8315. (c) Huang, F. H.; Jones, J. W.; Slebodnick, C.; Gibson, H. W. *J. Am. Chem. Soc.* **2003**, *125*, 14458–14464. (d) Jones, J. W.; Gibson, H. W. *J. Am. Chem. Soc.* **2003**, *125*, 7001–7004. (e) Clemente-Leon, M.; Pasquini, C.; Hebbe-Viton, V.; Lacour, J.; Dalla Cort, A.; Credi, A. *Eur. J. Org. Chem.* **2006**, 105–112.

(18) Affeld, A.; Hubner, G. M.; Seel, C.; Schalley, C. A. *Eur. J. Org. Chem.* **2001**, 2877–2890.

(19) Panman, M. R.; Bodis, P.; Shaw, D. J.; Bakker, B. H.; Newton, A. C.; Kay, E. R.; Brouwer, A. M.; Buma, W. J.; Leigh, D. A.; Woutersen, S. *Science* **2010**, *328*, 1255–1258.